Author's Accepted Manuscript

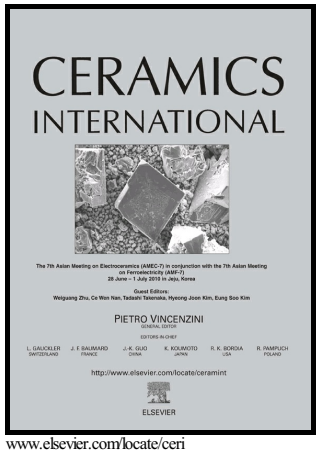

www.elsevier.com/locate/ceri

Perovskite $SrFe_{1-x}Ti_xO_{3-\delta}$ (x < = 0.1) cathode for Low Temperature Solid Oxide Fuel Cell

Naveed Mushtaq, Chen Xia, Wenjing Dong, G. Abbas, Rizwan Raza, Amjad Ali, Sajid Rauf, Baoyuan Wang, Jung-Sik Kim, Bin Zhu

PII: S0272-8842(18)30582-0
DOI: https://doi.org/10.1016/j.ceramint.2018.03.033
Reference: CERI17670

To appear in: *Ceramics International*

Received date: 3 January 2018
Revised date: 4 March 2018
Accepted date: 4 March 2018

Cite this article as: Naveed Mushtaq, Chen Xia, Wenjing Dong, G. Abbas, Rizwan Raza, Amjad Ali, Sajid Rauf, Baoyuan Wang, Jung-Sik Kim and Bin Zhu, Perovskite $SrFe_{1-x}Ti_xO_{3-\delta}$ (x < = 0.1) cathode for Low Temperature Solid Oxide Fuel Cell, *Ceramics International,* https://doi.org/10.1016/j.ceramint.2018.03.033

Perovskite $SrFe_{1-x}Ti_xO_{3-\delta}$ (x < = 0.1) cathode for Low Temperature Solid Oxide Fuel Cell

Naveed Mushtaq[1,2†], Chen Xia[3†], Wenjing Dong[1], G. Abbas[2] , Rizwan Raza[2**], Amjad Ali[2], Sajid Rauf [2], Baoyuan Wang[1], Jung-Sik Kim[5], Bin Zhu[1,3,4,5*]

[1]*Hubei Collaborative Innovation Center for Advanced Materials, Faculty of Physics and Electronic Science, Hubei University, Wuhan, Hubei 430062, P.R. China*

[2]*Department of Physics, COMSATS Institute of Information Technology, Lahore 54000, Pakistan*

[3]*Faculty of Materials Science and Chemistry, China University of Geosciences (Wuhan), Wuhan 430074, China*

[4]*Department of Energy Technology, Royal Institute of Technology, Stockholm, SE-10044, Sweden*

[5] *School of Aeronautical & Automotive Engineering, Loughborough University, Loughborough LE113TU, United Kingdom*

[*]Corresponding author, Bin Zhu, *Faculty of Materials Science and Chemistry, China University of Geosciences (Wuhan), Wuhan 430074, China*

Email address: binzhu@kth.se; zhubin@hubu.edu.cn

Department of Energy Technology, Royal Institute of Technology, Stockholm, SE-10044, Sweden

Tel.: +46 879 07 403; Fax: +46 8204161

Corresponding author, Rizwan Raza

Email address: rizwanraza@ciitlahore.edu.pk

†These authors contributed equally to this work.

Abstract

Stable and compatible cathode materials are a key factor for realizing the low-temperature (LT, ≤600 ˚C) operation and practical implementations of solid oxide fuel cells (SOFCs). In this study, perovskite oxides $SrFe_{1-x}Ti_xO_{3-\delta}$ (x < = 0.1), with various ratios of Ti doping, are prepared by a sol-gel method for cathode material for LT-SOFCs. The structure, morphology and thermo-gravimetric characteristics of the resultant SFT powders are investigated. It is found that the Ti is successfully doped into $SrFeO_{3-\delta}$ to form a single phase cubic perovskite structure and crystal structure of SFT shows better stability than $SrFeO_{3-\delta}$. The dc electrical conductivity and electrochemical properties of SFT are measured and analysed by four-probe and electrochemical impedance spectra (EIS) measurements, respectively. The obtained SFT exhibits a very low polarization resistance (R_p), 0.01 Ωcm^2 at 600◦C. The SFT powders using as cathode in fuel cell devices, exhibit maximum power density of 551 mW cm^{-2} with open circuit voltage (OCV) of 1.15V at 600◦C. The good performance of the SFT cathode indicates a high rate of oxygen diffusion through the material at cathode. By enabling operation at low temperatures, SFT cathodes may result in a practical implementation of SOFCs.

Keywords: LT-SOFCs; Perovskite Cathode; $SrFeTiO_{3-\delta}$; material stability; low polarization resistance; power density.

1 Introduction

To realize the practical implementations of solid oxide fuel cells (SOFCs), extensive efforts have been made to lower the operational temperature of the SOFCs from 1000◦C to 300-600◦C

[1]. Low operating temperature (LT) can reduce many issues in SOFCs, i.e. material degradation and gas sealing. It brings more choice of ceramic interconnects with cheap metals & materials, eventually realizing cost-effective SOFCs for commercialization [2]. Therefore, decrease in operating temperature is of great importance of the development of inexpensive and reliable SOFCs. However, at low temperatures it is extremely difficult to maintain sufficient electrochemical performance of each part (anode, electrolyte and cathode) for normal operation of SOFCs at LT [3-4]. Especially, in these part the cathode demands particular attention due to a larger activation energy of oxygen reduction reaction (ORR) caused by slower kinetic process at low temperatures. Therefore, conventionally, a high operational temperature is the major requirement for cathode in SOFCs to keep a sufficiently high reaction rate. For instance, typically conventional cathode $La_{1-x}Sr_xMnO_3$ (LSM) requires temperatures over 1000◦C [5]. To realize practical LT-SOFCs, it is very necessary to develop advanced cathode materials with high mixed ionic- electronic conduction, and good ORR activity rate for good electrochemical performance as well as good stability at LT circumstances.

In the past decade, a large number of mixed ionic and electronic conductors (MIECs) have been studied as cathode materials for intermediate temperature (IT) SOFCs [6, 7]. Among the perovskite oxides, the materials with high mixed ionic and electronic conductivity exhibited tremendous prospective potential for LT-SOFCs [8]. The perovskites have a general formula ABO_3, where A, B are distinct metal cations. The ABO_3 perovskite can be doped either on A site or B site to adjust its electrical properties. In general, a cation having larger ionic radius occupies the A-site, and the cation with smaller radius is on the B-site [9, 10]. In most of the perovskite cathodes, A site cations are alkaline and rare earth elements such as La, Sr, Ca, and Ba, and B site cations are reducible transition metal such as Fe, Co, Mn and Ni. Among these perovskite

materials, LSM is the most widely used cathode in SOFCs, because of its high electronic conductivity, good electrochemical activity for ORR, and high thermal stability [11]. Some other typical Fe-based perovskite oxides, such as $La_{0.8}Sr_{0.2}FeO_{3-\delta}$, $Ba_xSr_{1-x}FeO_{3-\delta}$, and $Sm_{0.5}Sr_{0.5}FeO_{3-\delta}$ are also commonly proposed as cathode materials for IT-SOFCs [12]. It is studied in the past decade that many iron-based oxides have emerged in the form of perovskite structure. These Fe-doped perovskite oxides have attracted much attention, as iron is naturally abundant and cost-effective. In addition, iron oxides are reported to possess effective catalytic activity for ORR and are structurally stable when associated with the flexible coordination numbers of the iron cations surrounded by oxygen anions in the perovskite structure. As another representative, perovskite $SrFeO_{3-\delta}$ exhibits high mixed ionic and electronic conductivity and Mo-doped $SrFeO_{3-\delta}$ shows good stability in a wide range of oxygen partial pressures and has been demonstrated as a redox stable electrode for SOFCs [13]. The thermal expansion coefficient is also key parameter for the thermally stable and long term operation of the SOFCs. The thermal expansion coefficient (TEC) of Ti-doped $SrFeO_{3-\delta}$ (approximately 25.9×10^{-6}) is reported to be thermally compatible with Sm-doped ceia (SDC) electrolyte [14]. It has also been indicated that by doping Ti into the B site $SrFeO_{3-\delta}$ lattice can improve the structure stability and realize good electrochemical performance [15]. These results promote interests in studying doped $SrFeO_{3-\delta}$ perovskites as advanced cathode family materials.

In this work, the authors prepared a Ti-doped $SrFeO_{3-\delta}$ perovskite $SrFe_{1-x}Ti_xO_{3-\delta}$ ($x <= 0.1$) with various Ti-doping ratios, and evaluated them as cathode materials for LT-SOFCs. The phase structure and morphology of the prepared materials were characterized. The electrical and electrochemical properties of the prepared materials are also investigated.

2 Experimental

2.1 Synthesis of SFT by wet chemical method

$SrFe_{1-x}Ti_xO_{3-\delta}$ (x < = 0.1) powders were synthesized by sol-gel method. The stoichiometric amounts of strontium nitrate hexa-hydrate $Sr(NO_3)_2 \cdot 6H_2O$ (Sigma Aldrich 99.99%), iron nitrate nona- hydrate $Fe(NO_3)_3 \cdot 9H_2O$ (Sigma Aldrich 99.99%) and titanium dioxide (TiO_2, Sigma Aldrich 99.99%) were used. An appropriate molar ratio of strontium and iron nitrates were dissolved into distilled water, while TiO_2 was dissolved into hot concentrated (66%) H_2SO_4) and NH_4OH were added to form neutral solutions respectively. Both solutions were combined to form an aqueous solution to the material after 30 minutes continuous stirring. Citric acid was then added with 25 % of total moles of SFT into the solution. Following which, these solutions were stirred (200 rev/min) and heated continuously at 80◦C for four hours to obtain gel. Subsequently, the resulting gel was dried at 200 ^{o}C for 3 hours and ground in mortar pestle to attain powder, followed by calcinations at 1100◦C for 5 hours. Finally, the powders were grounded adequately again for characterizations and cell fabrication.

2.2 Preparation of single cell and fabrication of fuel cell devices

For fabrication of fuel cells, the powders of the anode, electrolyte and cathode were filled one by one into a die, and compressed under a pressure of 220 MPa using a CARVER Hydraulic press (USA). The thickness of the fuel cell was 1.5 mm and the active area was 0.64 cm^2. $Sm_{0.2}Ce_{0.8}O_2$ (SDC) [16], LiNiCuZn-oxide [17], and $SFe_{1-x}Ti_xO_{3-\delta}$ were used as the electrolyte, anode and cathode, respectively. The fabricated cells were then sintered at 700◦C for 1 hour before measurements. The silver paste was used as current collector on both sides of the cells. For DC four Probe conductivity measurements, the samples were fabricated into pellets with 2 mm in thickness and 13 mm in diameter at 220 MPa.

2.3 Material characterizations and electrochemical measurements

The phase structure of the synthesized $SrFe_{1-x}Ti_xO_{3-\delta}$ (x < = 0.1) powders was characterized using X-ray diffraction ((PAN analytical with Cu K_α radiation, λ=1.5418 Å) in 2θ scan range of 0-90˚ with a scanning step of 0.02^o. All refinement for obtained XRD was studied by MJAD 6.5 software. The surface morphology of the synthesized SFT was studied by scanning electron microscopy (SEM, Vega 3, LMU, Tescan). Images were captured at different magnifications with accelerated voltage of 10 kV. Thermo-gravimetric analysis (TGA) was employed to measure the weight loss or gain studies using TA Instruments (SDT Q 600 V 8.2 build 100) in temperature range of 25- 800◦C in the presence of Nitrogen (heating rate: 15◦C/min). The particle surface area and pore size of samples were measured through surface area and porosity analyzer Brunauer–Emmett–Teller (BET; Tristar).

Electrochemical impedance spectroscopy (PARSTAT 4000 EIS Analyser) was used for the measurements of electrochemical performance under the cell open circuit voltage (OCV) mode (Working and Sense, Reference and Common). The measurements were carried out in frequency ranges from 0.1Hz-1MHz with an AC applied signal voltage of 10mV in amplitude in temperature range 500-600◦C. ZSIMPWIN software was used to simulate the experimental EIS data based on equivalent circuits. DC conductivity measurements were carried out at 350-650◦C using four-probe method by KEITHLEY 2450 source meter and simulated by Kick Start software. The electrical conductivity is calculated from equation σ_{dc} =L/RA, where L is the thickness (length), R is the resistance and A is the active area of the pellet. The fuel cells were tested using H_2 - air as fuel and oxidant, respectively, with a flow rate of 100ml/min. The voltage and current was recorded for I-V (current voltage) and I-P (current density-power density) characteristics.

3 Results and discussions

3.1.1 Crystal & Microstructure

The X-ray diffraction patterns of the as-prepared $SrFe_{1-x}Ti_xO_{3-\delta}$ (x < = 0.1) samples are shown in Fig. 1. The characteristic peaks in Fig. 1(a) manifest the single phase cubic perovskite structures. No other phase formation can be observed in all compositions, suggesting that Ti was successfully doped into B-site to replace partial Fe ions. The refinements were calculated using MJAD 6.5 software according to JCPDS File No. 33-0677.The crystallite size was calculated using Scherer equation,

$$D = K\lambda/L(cos\theta)$$

Where D is the crystallite size, λ is the wavelength and L is the full width half maxima (FWHM). The average crystallite size of 44 nm is calculated for sample with x = 0.1. The XRD patterns characteristic peaks show slight shift towards the lower angle with the increase of titanium contents, indicating a lattice parameter change by expanding the unit cell structure. The unit cell parameters for the samples are calculated, revealing increasing value from 3.86405 Å (x=0) to 3.89605 Å (x=0.1), as summarized in table 1 and presented in Fig.1(c). The lattice parameter of the unit cell is linearly increased with the titanium contents, which may be attributed to the difference in their ionic radii and possible reduction of Fe^{4+} to Fe^{3+} and Ti^{4+} to Ti^{3+}, obeying Vegard's law [18,19].

Fig.2 presents the SEM micrograph of the resultant $SrFe_{1-x}Ti_xO_{3-\delta}$ (x < = 0.1) powders. The figure 2(a-c), correspond to Ti contents with x = 0, 0.05 and 0.075 powders, respectively. The average grain size is calculated by ImageJ software to be 2.98, 0.953 and 0.5 µm,

respectively for the three samples. To check the presence of Ti contents into $SrFeTiO_{3-\delta,}$ EDX is used. Fig. 2b shows the SEM image and EDX elements mapping for all the elements present in $SrFe_{0.9}Ti_{0.1}O_{3-\delta.}$ It can be seen from the images that the grain size is obviously affected with the introduction of Ti, decreasing along with the increase of Ti content, which suggests that the substitution of Ti for Fe restrains the grain growth [14]. The grain size change leads to a more porous morphology, which is more suitable for gas diffusion when the samples are used as cathodes of fuel cells. It can be seen that all the elements are distributed homogenously at all the surface.

3.1.2 Thermo-gravimetric Analysis (TGA)

Thermodynamic analysis is essential for predicting the long-term stability of perovskite cathode material besides the electrical conduction and structural characteristics. The TGA of $SrFe_{1-x}Ti_xO_{3-\delta}$ ($x <= 0.1$) was performed to study the mechanisms of decomposition and the formation of the final desired phase. Fig. 3 shows thermal analysis (TA) plot, consisting of three regions spanned over the range of 25-290◦C, 290-450◦C, and 450-800◦C, respectively. It can be seen from the plot that there is a large weight loss in region-I due to the physically desorption of absorbed water and chemical water in nitrates which evaporate in this temperature region [20]. In region-II, it can be seen that the weight loss is associated with the decomposition of the chemical compounds, e.g. nitrates [21].In region-III, two ranges can be discerned: a) from 450-500◦C, the combustion process of material has occurred and the required oxide phase formation has commenced; b) a second weight loss stage is observed from 500-800◦C, probably due to the loss in lattice oxygen. The weight losses increasing with titanium contents could be attributed to the difference in initial oxygen vacancy content or superior reduction of titanium in the prepared

cathode material [22]. Comparatively, it is found $SrFe_{1-x}Ti_xO_{3-\delta}$ with x = 0.1 exhibits markedly better thermodynamic stability than the other three samples.

3.1.3 BET (Brunaurr-Emmett-Teller)

For further investigation, the pore sizes of powders were carried out using BET analysis. The data obtained from BET studies are summarized in table 1. Both pore size and BET surface area show an increasing trend with the increase of x, corresponding to the decrease of particle size. These results provide good argument with the above SEM results.

3.2 Electrical conductivity

Sufficient electrical conductivity is the major parameter for better performance of cathode material. Four-probe dc conductivity measurements of $SrFe_{1-x}Ti_xO_{3-\delta}$ (x < = 0.1) were carried out in air in the temperature range of 350-650◦C. The results are presented in Fig. 4 in form of Arrhenis plot (1000/T (K) vs. Ln σ T). Generally, in MIECs perovskite, the electronic conductivity can be considered several orders of magnitude high than the ionic conductivity [18]. It is clear from the plot that the electrical conductivity gradually improves with the increase of temperature, which primarily reflects the property of electronic conduction of the semiconductor. The electrical conductivity is observed to be reduced with increasing titanium content. The maximum conductivity obtained was 9 Scm^{-1} for $SrFeO_{3-\delta}$, at 650◦C, but gradually reduced to 2.25 Scm^{-1} for $SrFe_{0.9}Ti_{0.1}O_{3-\delta}$. This decrease in electrical conductivity can be attributed to the reduction in charge carriers i.e., the ratio of Fe^{4+}/Fe_{total} due to increasing titanium content. Additionally, the corresponding activation energy (E_a) for electrical conductivity was calculated based on Arrhenius relationship $\sigma = (\sigma_o/T) \exp(-E_a/RT)$, where σ is the conductivity, σ_o is the pre-exponential constant, E_a is the activation energy, R is the universal gas constant and T is the

process temperature [24, 25]. As a result, the calculated activation energy values for the prepared SFT samples are 59.6 J/mol, 56.02 J/mol, 54 J/mol and 48.79 J/mol for x = 0, 0.05, 0.075 and 0.1, respectively, at 350-650◦C. The lowest activation energy is observed in $SrFe_{1-x}Ti_xO_{3-\delta}$, (x = 0.1), as compared to other Ti contents. Thus, it provides support that the sample with x = 0.1 is a good material for cathode at low-temperature operation.

3.3 EIS Analysis

To investigate the effect of Ti-doping contents on the electrochemical performance, symmetrical cells with $SrFe_{1-x}Ti_xO_{3-\delta}$ (x < = 0.1) electrodes were constructed on $Sm_{0.2}Ce_{0.8}O_2$ (SDC) electrolyte (SFT/SDC/SFT). The oxygen reduction reaction (ORR) capabilities of both Ti-doped and un-doped perovskite oxides were studied by electrochemical impedance spectroscopy (EIS). Fig. 5(a-d) present the typical impedance spectra for the symmetric cells of SFT|SDC|SFT measured in air over a temperature range from 500-600◦C. The EIS data was fitted based on equivalent circuit, i.e., $L/R_1/(R_2Q)$ (Fig. 5g) using ZSIPWIN software. It is clearly seen that each EIS data fits well with the equivalent circuit. The R_1 corresponds to the ohimic resistance of electrolyte, devices and system wires simultaneously. The corresponding cathode polarization resistance R_p can be obtained based on the fitting results of R_2 ($Rp=R_2$) [26-32]. The calculated R_p values of all four cathodes at various temperatures from EIS are presented in Fig. 5f, the polarization resistance values of the $SrFe_{1-x}Ti_xO_{3-\delta}$ (x < = 0.1) electrodes are 0.625, 0.283, 0.096 and 0.01 Ω cm^2 at 600◦C, respectively. This indicates that the R_p of SFT (x = 0.05, 0.075, 0.1) is less than that of $SF_{1-x}Ti_xO_{3-\delta}$ (x=0) at 600◦C. At other temperatures, the Ti-doped oxides also exhibit lower polarization resistance than the parent $SFO_{3-\delta}$, and the $SrFe_{1-x}Ti_xO_{3-\delta}$ (x = 0.1) electrode shows the lowest R_p at each temperature. These results confirm that the catalytic activity for ORR of $SFO_{3-\delta}$ can be improved through proper Ti doping. Fig. 5(e) describes the

comparison of EIS results for all four cathodes at 600◦C. The ohmic resistance from the electrolyte has been subtracted for the sake of clarity. The Arrhenius plot of R_p is presented in Fig. 5 (f). It can be clearly seen in Fig. 5 (f) that the R_p decreased with increase in temperature and Ti content. Table 3a lists the summary of EIS fitted results. It should be noted that the polarization resistance values of $SrFe_{1-x}Ti_xO_{3-\delta}$ (x = 0.1) cathode are comparable to many reported B-site Ti-doped SF cathodes, as listed in table 3b.

3.4 Fuel Cell Performance

The fuel cell performance of $SrFe_{1-x}Ti_xO_{3-\delta}$ (x < = 0.1), as cathodes was studied using cell configurations of LiNiCuZn/SDC/SFT cells. Fig.6 (a) shows typical current-voltage (I-V) and current-power (I-P) characteristics of the cells with $SrFe_{1-x}Ti_xO_{3-\delta}$ (x < = 0.1) measured at 600◦C. The best performance of maximum power density of 551 mW cm^{-2} and open circuit voltage (OCV) of 1.15V are achieved at 600◦C for Ti contents with x=0.1. Fig. 6 (a) shows the comparison of power densities for all compositions at 600◦C. The peak power densities of 551 mW cm^{-2}, 442 mW cm^{-2}, 332 mW cm^{-2} and 236 mW cm^{-2} are obtained for $SrFe_{1-x}Ti_xO_{3-\delta}$ (x < = 0.1), respectively. Considering the results obtained at 600◦C for SFT cathode, we further studied cell with best performance at various temperatures, which are presented in fig. 6 (b). Summary of the fuel cell performances for different compositions is presented in Table 4a. It should be noticed that both the cell open circuit voltages (OCVs) and peak power output are dependent on the Ti content. The increase in Ti content can directly enhance OCV values and corresponding power outputs. This indicates clearly that the Ti doping can strongly promote ORR process, thus reducing cathode polarization resistance significantly as proved by the results from the EIS discussions. The Table 4 summarises the authors' obtained cell performance in comparison with previous reported $SrFeTiO_{3-\delta}$-based perovskite cathodes listed in table 4b. Consequently, it can

be established that the fuel cell based on $SrFe_{1-x}Ti_xO_{3-\delta}$ (x=0.1) fabricated here demonstrates better performance even at lower temperature.

4. Conclusions

In summary, the $SrFe_{1-x}Ti_xO_{3-\delta}$ (x < = 0.1) was successfully prepared using a sol-gel method. The prepared samples show a single phase cubic perovskite structure. It was observed that lattice parameters increase with increasing titanium concentration. The electrical conductivity is decreased by increasing the dopant content of titanium. The maximum conductivity is 9 Scm^{-1} at 600◦C for $SrFeO_{3-\delta}$, whilst it decreases to 2.25 Scm^{-1} for the sample with x = 0.1. The $SrFe_{1-x}Ti_xO_{3-\delta}$ Cathode material possessed the polarization resistance of 0.01 Ωcm^2 for x = 0.1 at 600◦C. The pore size is increased with higher titanium content, i.e. the titanium concentration increases the porosity of the material. This can fulfil the cathode requirement and thus highly benefit the charge diffusion and ORR processes resulting in very low polarization resistance and high cell performance at low temperatures. Therefore, these results suggest that $SrFe_{0.9}Ti_{0.1}O_{3-\delta}$ can be considered for highly promising cathode material for advanced LT-SOFCs.

Acknowledgement

This work was supported by National Natural Science Foundation of China (NSFC) under the grant # 11604088 and NSFC 51772080. I would also like to thanks COMSAT Institute of information Technology (CIIT) Lahore Pakistan for providing research facilities.

References

[1] Tauqeer Abbas, Aqeel Ahmed Bazmi, Abdul Waheed Bhutoo and Gholamreza Zahedi, Greener energy: Issues and challenges for Pakistan-geothermal energy prospective, Renewable and Sustainable Energy Reviews 31 (2014) 258-269.

[2] M. Ashraf Chaudhry, R. Raza, S.A. Hayat, Renewable energy technologies in Pakistan: prospectus and challenges, Renewable and Sustainable Energy Reviews 13 (2009) 1657-1662.

[3] Rizwan Raza, Nadeem Akram, Muhammad Sufyan Javed, Asia Rafique, Kaleem Ullah, Amjad Ali, M. Saleem and Riaz Ahmed, Fuel cell technology for sustainable development in Pakistan-An over view, Renewable and Sustainable Energy Reviews 53 (2016) 450-461.

[4] Chunwen Sun, Rob Hui, Justin Roller, Cathode materials for solid oxide fuel cell: a review, Solid State Electrochemistry 14 (2010) 1125-1144.

[5] Takehiko Takahashi, High Conductivity Solid Ionic Conductors, Recent Trends and Applications, World Scientific Singapore (1998) 630-635.

[6] Dr Stephen, J.Skinner, Recent advances in perovskite-type materials for SOFC cathodes, Fuel Cells Bulletin 33 (2001) 6-12.

[7] J Skinner, John A Kilner, Oxygen ion conductors. Materials Today 6 (2003) 30-37.

[8] Anna Lashtabeg, Jesues Canales-Vazquez, John T.S. Irvine, John L. Bradley, Structure, Conductivity and Thermal Expansion Studies of redox stable Rutile Niobium Chromium Titanates in Oxidizing and Reducing Conditions, Chemistry of Materials 21 (2009) 549-3561.

[9] J Molenda, K Świerczek, M Molenda, J Marzec, Electronic structure and reactivity of $Li_{1-}\boldsymbol{x}Mn_2O_4$ cathode, Solid State Ionic 135 (2000) 53-59.

[10] Joseph Fehribach, Ryan O'Hayre, Triple Phase Boundaries in Solid-Oxide Cathodes, Journal on Applied Mathematics 70 (2009) 510-530.

[11] Huber, T. M., The relevance of different oxygen reduction pathways of $La_{0.8}Sr_{0.2}MnO_{3-\delta}$ (LSM) thin film model electrodes, *Journal of the Electrochemical Society* 162 (2015) 229-242.

[12] Jun A, Yoo S, Gwon OH, Shin J, Kim G, Thermodynamic and electrical properties of $Ba_{0.5}Sr_{0.5}Co_{0.8}Fe_{0.2}$ $O_{3-\delta}$ and $La_{0.6}$ $Sr_{0.4}Co_{0.2}$ $Fe_{0.8}O_{3-\delta}$ for intermediate-temperature solid oxide fuel cells, Electrochimica Acta 89 (2013) 372-376.

[13] Y. Niu, W. Zhou, J. Sunarso, L. Ge, Z. Zhu, Z. Shao, Investigation into the effect of Si doping on the cell symmetry and performance of $Sr_{1-y}Ca_yFeO_{3-\delta}$ SOFC cathode materials, J. Mater. Chem. 20 (2010) 9619–9622.

[14] Xiuling Yu, Juanjuan Fan, Xue Li, Performance optimization of $SrFe0._{95}Ti_{0.05O3-\delta}$ cathode for intermediate temperature SOFC, Ceramics International 40 (2014) 13627-13634.

[15] V.V Kharto, A. P Viskup, A.V Kovalevsky, J.R Jurado, E.N Naumovich, Oxygen ionic conductivity of Ti-containing strontium ferrite, Solid State Ionics 133 (2000) 57-65.

[16] Mingfei Liu, Dong Ding, Yaohui Bai, Ting He, Meilin Liu, An Efficient SOFC Based on Samaria-Doped Ceria (SDC) Electrolyte, Electrochem. Soc. 159 (2012) 661-665.

[17] Yufeng Zhao, Jing He, Liangdong Fan, Wei Ran, Chunming Zhang, Dawei Gao, Chengyang Wang, Faming Gao, Synthesis and characterization of hierarchical porous LiNiCuZn-oxides as potential electrode materials for low temperature solid oxide fuel cells, international journal of hydrogen energy 38 (2013) 16558-16562.

[18] Harumi Yokokawa, Natsuko Sakai, Tatsuya Kawada and Masayuki Dokiya, Thermodynamic stabilities of perovskite oxides for electrodes and other electrochemical materials, Solid State Ionics 52 (1992) 43-56.

[19] Harumi Yokokawa, Tatssuya Kawada, Masayuki Dokiya, Thermodynamic Regularities in Perovskite and K_2NiF_4 Compounds, Journal of the American Ceramic Society 72 (1989) 52-53.

[20] Shuyan Li, ZheLu, Xiqiang Huang, Bo Wei and Wenhui Su, Electrical and thermal properties of $(Ba_{0.5}Sr_{0.5})_{1-x}Sm_xCo_{0.8}Fe_{0.2}O_{3-\delta}$ perovskite oxides, Solid State Ionics 178 (2007) 417-422.

[21] Yousef M. Al-Yousef and Mohammad Ghouse, Synthesis of $Ba_{0.5}Sr_{0.5}Co_{0.2}Fe_{0.8}O_3$(BSCF) nano-ceramic Cathode Powders by Sol-Gel Process for Solid Oxide Fuel Cell (SOFC) Application, World Journal of Nano Science and Engineering 1 (2011) 99-107.

[22] Peter I. Cowin, Conductivity and redox stability of perovskite oxide, Solid State Science 46 (2015) 62-70.

[23] Peter I. Cowin, RongLan, ChristopheT.G.Petit, Dongwei Du, Kui Xie, Huanting Wang, Shanwen Tao, Conductivity and redox stability of new perovskite oxides $SrFe_{0.7}TM_{0.2}Ti_{0.1}O_{3-\delta}$(TM = Mn, Fe, Co, Ni, Cu), Solid State Ionics 301 (2017) 99–105.

[24] Muhammad Sufyan Javed, Rizwan Raza, Zishan Ahsan, M. Shahid Rafique, Shamaila Shahzadi , S.F. Shaukat, Nusrat Shaheen, Muhammad Saeed Khalid, Hu Chengou, Bin Zhu Electrochemical studies of perovskite cathode material for direct natural gas fuel cell, International journal of hydrogen energy 41 (2016) 3072-3078.

[25] Costas Sikalidis. Advance in ceramics- synthesis and characterizations, processing and specific Applications, *InTech* 10 (2011) 425-430.

[26] Virkar, A., The role of electrode microstructure on activation and concentration polarizations in solid oxide fuel cells, Solid State Ionics 131 (2000) 189-198.

[27] B. Wei, Z. Lu, X. Q. Huang, M. L. Liu, N. Li, and W. H. Su, Synthesis, electrical and electrochemical properties of $Ba_{0.5}Sr_{0.5}Zn_{0.2}Fe_{0.8}O_{3-\delta}$ perovskite oxide for IT-SOFC cathode Journal of Power Sources 176 (2008) 1-8.

[28] Y.J. Leng, S.H. Chan, K.A. Khor, S.P. Jiang, Performance evaluation of anode-supported solid oxide fuel cells with thin film YSZ electrolyte, International journal of Hydrogen Energy 29 (2004) 1025-1033.

[29] D. Xie, W.Guo, R. Guo, Z. Liu, D. Sun, L. Meng, M. Zheng, and B. Wang. Synthesis and Electrochemical Properties of $BaFe_{1-x}Cu_xO_{3-\delta}$ Perovskite Oxide for IT-SOFC Cathode, ORIGINAL RESEARCH PAPER FUEL CELL 00 (2016) 1-10.

[30] Jung Hyun Kim, Mark Cassidy, John T.S. Irvine, Joongmyeon Bae, Electrochemical Investigation of Composite Cathodes with $SmBa_{0.5}Sr_{0.5}Co_2O_{5+\delta}$ Cathodes for Intermediate Temperature-Operating Solid Oxide Fuel Cell, Chemistry of Materials 22 (2010) 883–892.

[31] Shizhong Wang, Tong Chen, and Shengpei Chen, Kinetics of Oxygen Reduction over $Sm_{0.5}Sr_{0.5}CoO_3$, Supported on $La_{0.9}Sr_{0.1}Ga_{0.8}Mg_{0.2}O_3$, Journal of The Electrochemical Society 151(2004) 1461-1467.

[32] Maria Escudero, Ainara Aguadero, José Antonio Alonso, L. Daza, A Kinetic Study of Oxygen Reduction Reaction on La_2NiO_4 Cathodes by Means of Impedance Spectroscopy, Journal of Electroanalytical Chemistry 611 (2007) 107-116.

[33] Yubo Chen, Baoming Qian, Sidian Li, Yong Jiao, Moses O. Tade, and Zongping Shao, The influence of impurity ions on the permeation and oxygen reduction properties of Ba0.5Sr0.5Co0.8Fe0.2O3δperovskite, Journal of Membrane Science 449 (2014) 86–96.

[34] Guangming Yang, Jian Shen, Yubo Chen, Moses O. Tade, Zongping shao, Cobalt-free $Ba_{0.5}Sr_{0.5}Fe_{0.8}Ti_{0.1}O_{3-\delta}$ as a bi-functional electrode material for solid oxide fuel cell, Journal of Power Sources 298 (2015) 184-192.

[35] Sungmee Cho, Daniel Fowler, Elizabeth C. Miller, J.Scott Cronin, Kenneth R. Poeppelmeier, Scott A. Barnett, Fe-substituted $SrTiO_{3-\delta}$-$Ce_{0.9}Gd_{0.1}O_2$ composite anodes for solid oxide fuel cells, Energy Environ. Sci. 6 (2013) 1850-1857.

[36] Weidong Li, Ye Cheng, Qingjun Zhou, Tong Wei, Zepeng Li, Huiyu Yan, Zheng Wang, Xue Han, Evaluation of double perovskite $Sr_2FeTiO_{6-\delta}$ as potential cathode or anode materials for intermediate-temperature solid oxide fuel cells, Ceramics International 41 (2015) 12393-12400.

[37] XiulingYu, Wen Long, Fangjun Jin, Tianmin He, Cobalt-free perovskite cathode materials $SrFe_{1-x}Ti_xO_{3-\delta}$ and performance optimization for intermediate-temperature solid oxide fuel cells, Electrochimica Acta, 23 (2014) 426-434.

Figures

3.1.1 Crystal & Microstructure

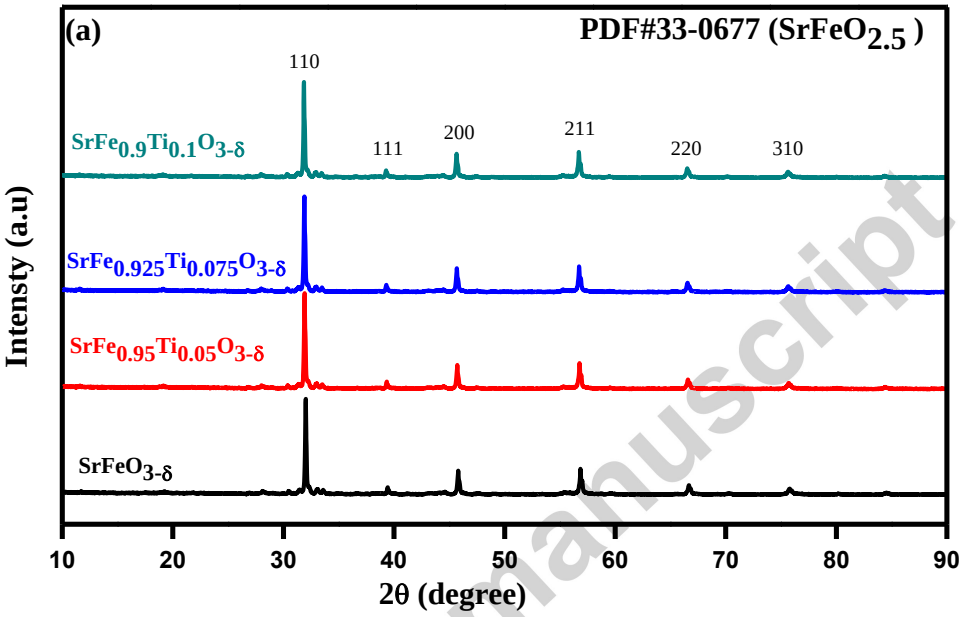

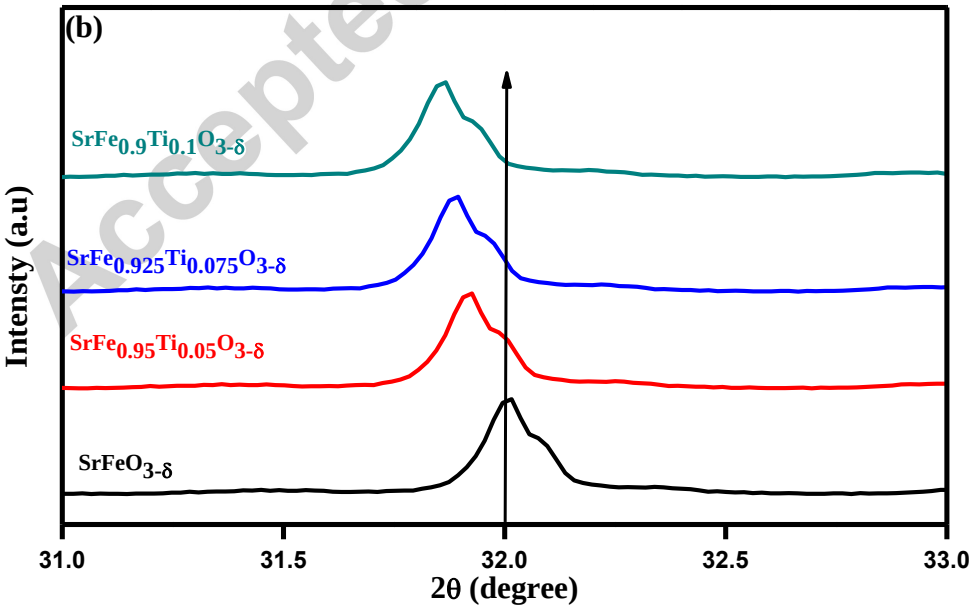

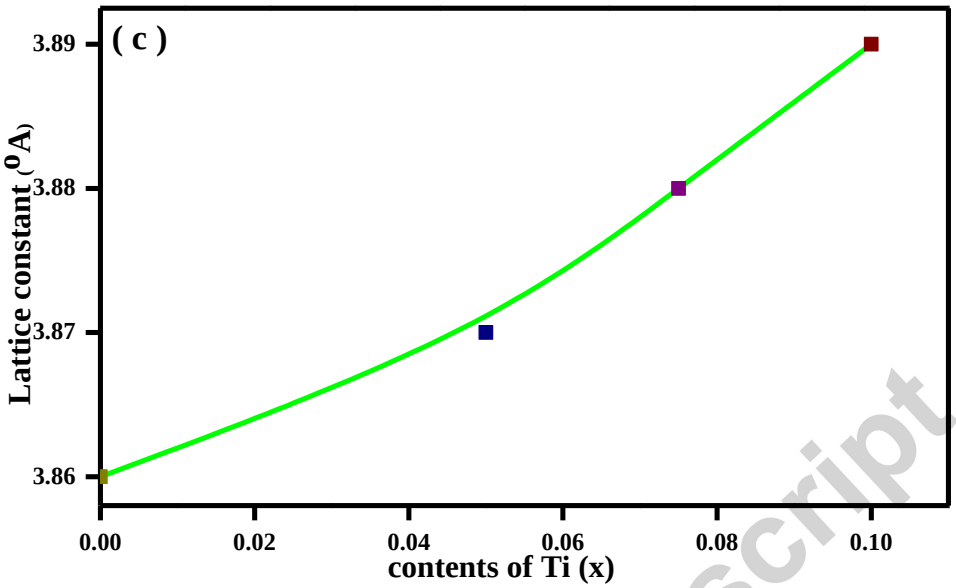

Fig. 1 (a) X-ray diffraction pattern of respective powders of $SrFe_{1-x}Ti_xO_{3-\delta}$ sintered at 1100°C in air for 5 hour, (b) peaks shifting in diffraction pattern with different Ti contents, (c) change in unit cell parameters with various Ti contents.

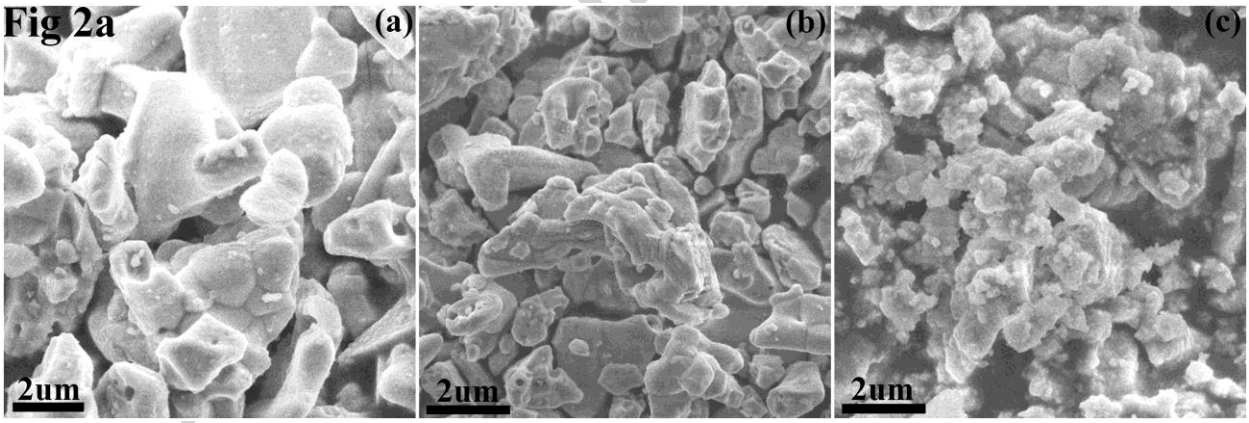

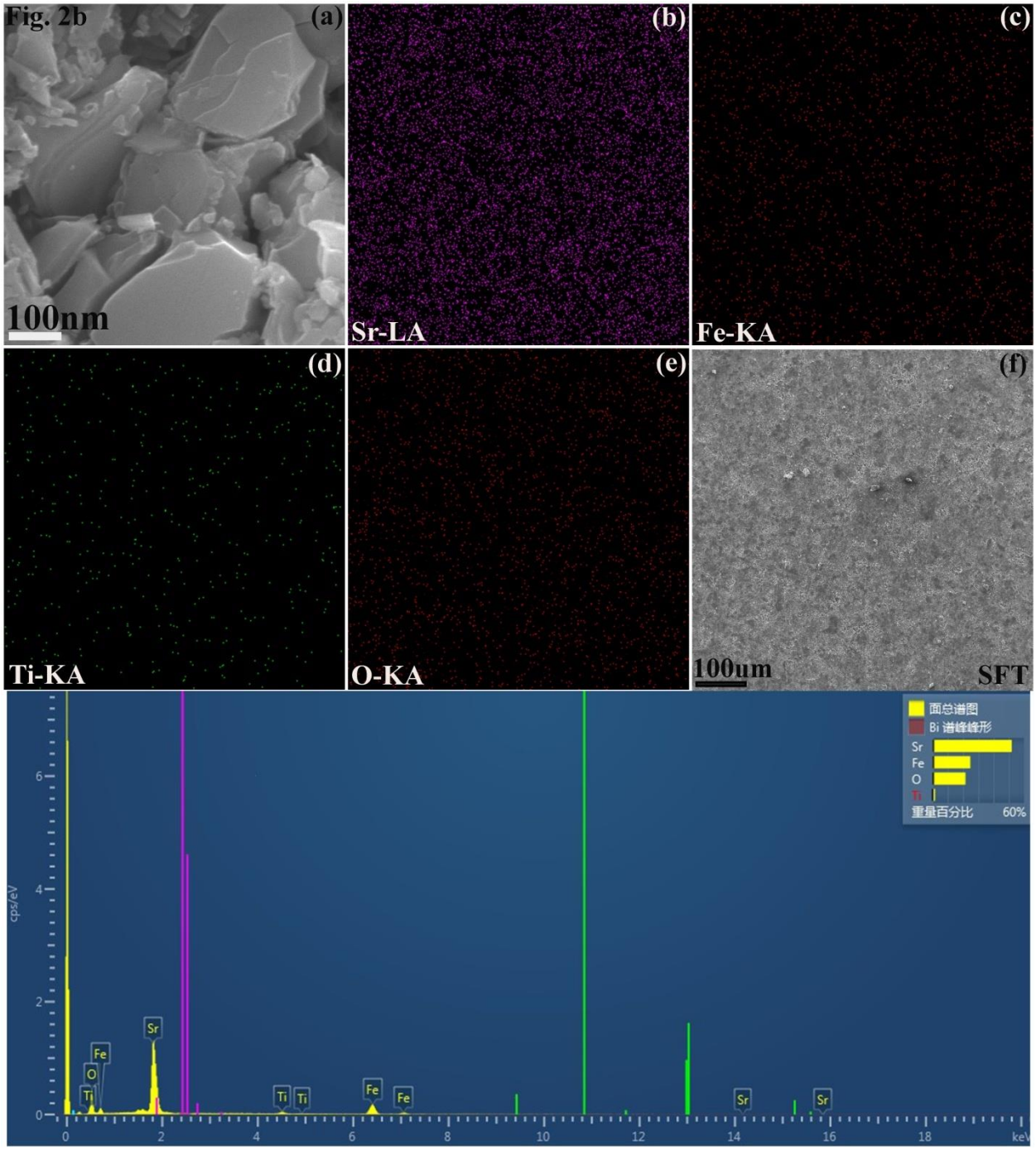

Fig. 2 (a) SEM micrograph of $SrFe_{1-x}Ti_xO_{3-\delta}$ samples with x=0, 0.05 and 0.075 after calcinations at different magnifications, (b) SEM image, EDX mapping of all the elements for $SrFe_{1-x}Ti_xO_{3-\delta}$ (x = 0.1)

3.1.2 Thermo-gravimetric Analysis (TGA)

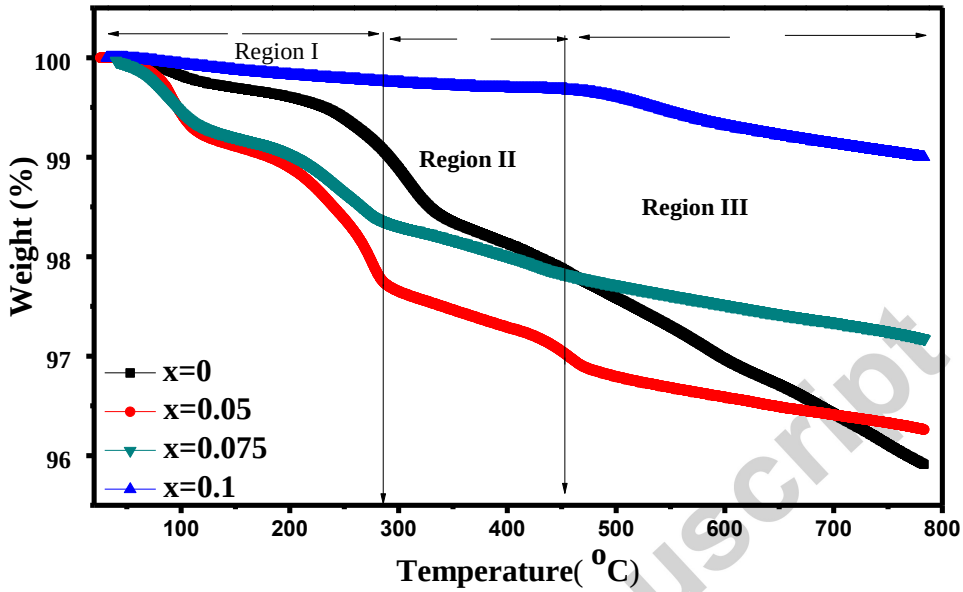

Fig. 3 Thermo-gravimetric analysis (TGA) curve for the respective $SrFe_{1-x}Ti_xO_{3-\delta}$ (x < = 0.1) from 25◦C - 800◦C in N_2/air.

3.2 Electrical conductivity

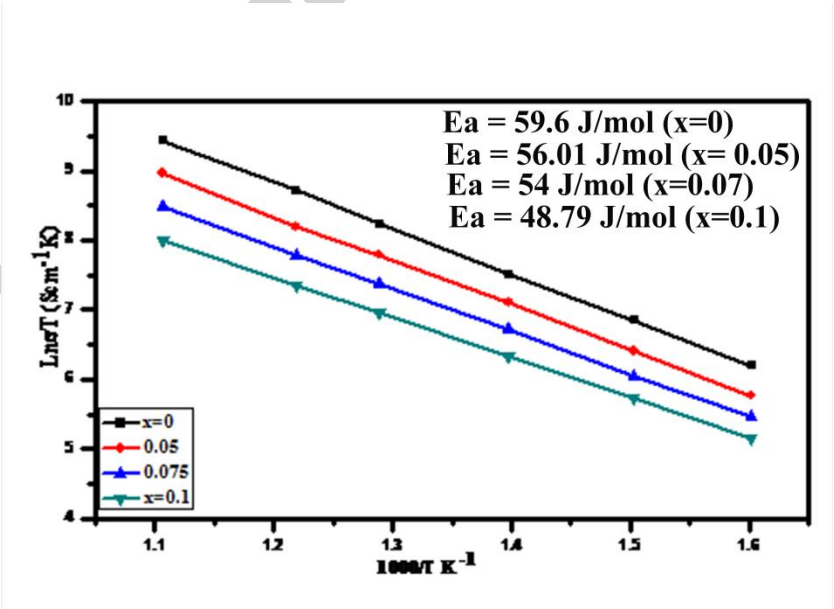

Fig. 4 Arrhenius plot of dc electrical conductivities and calculated activation energy values are inserted for $SrFe_{1-x}Ti_xO_{3-\delta}$ (x < = 0.1) from 350◦C - 650◦C in air

3.3 EIS Analysis

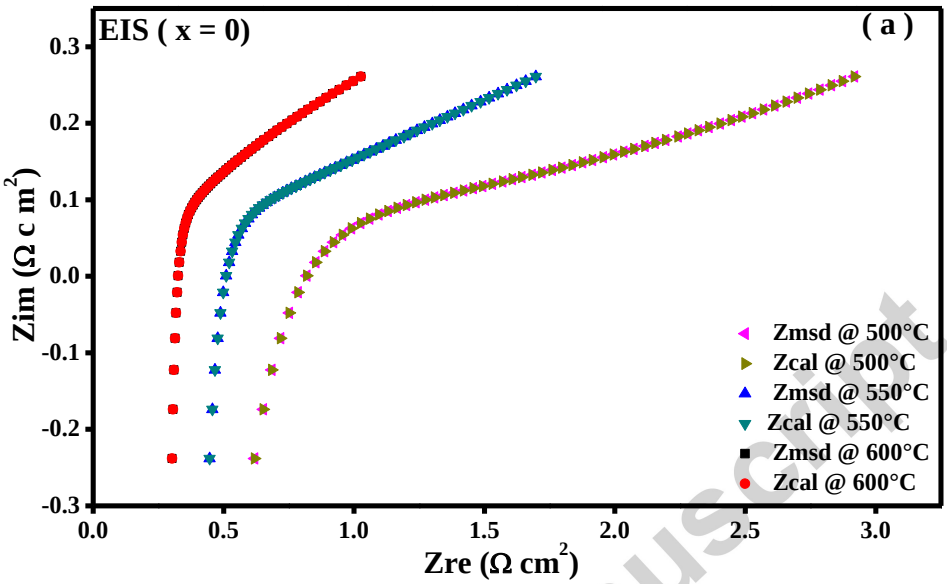

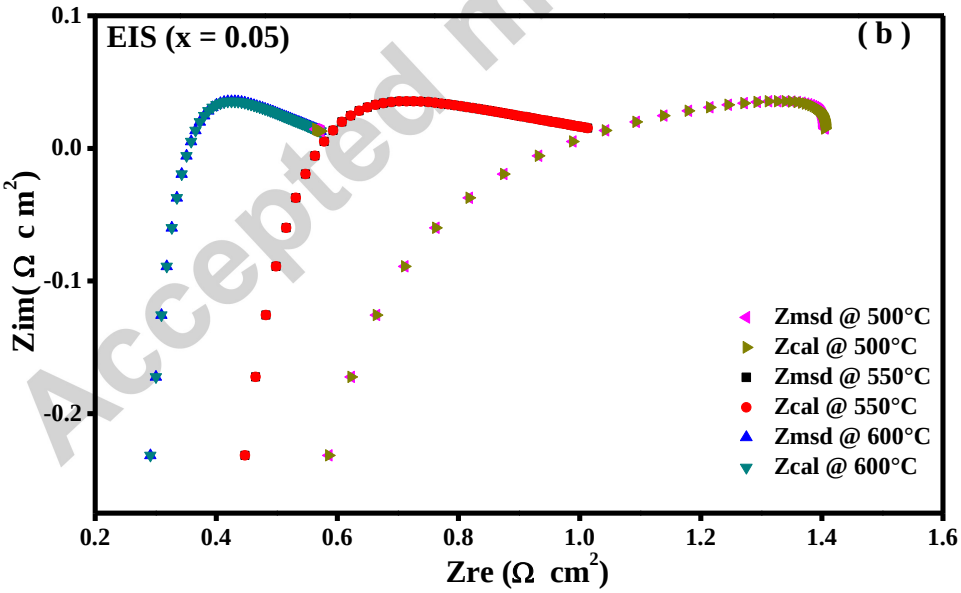

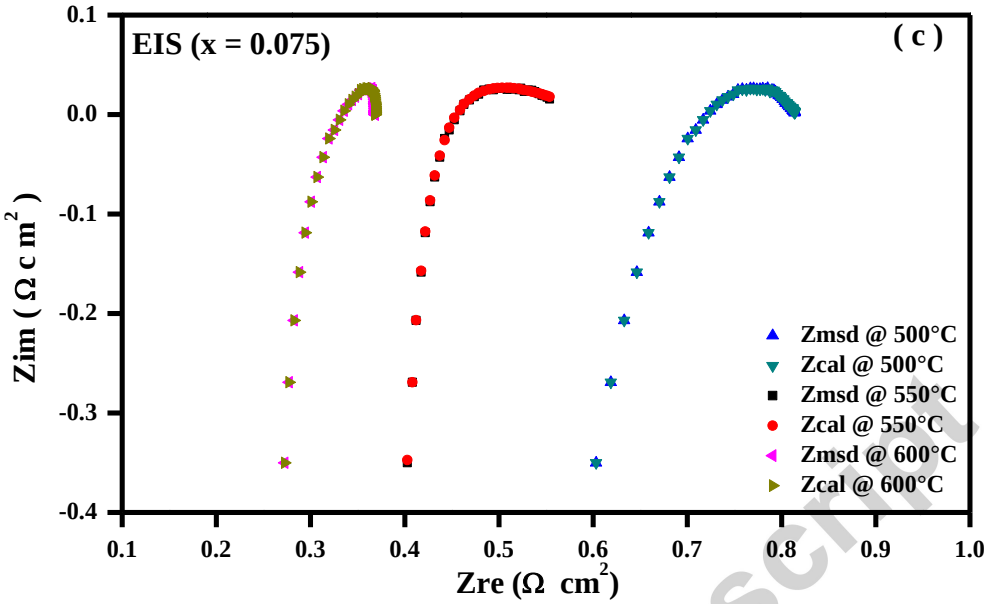

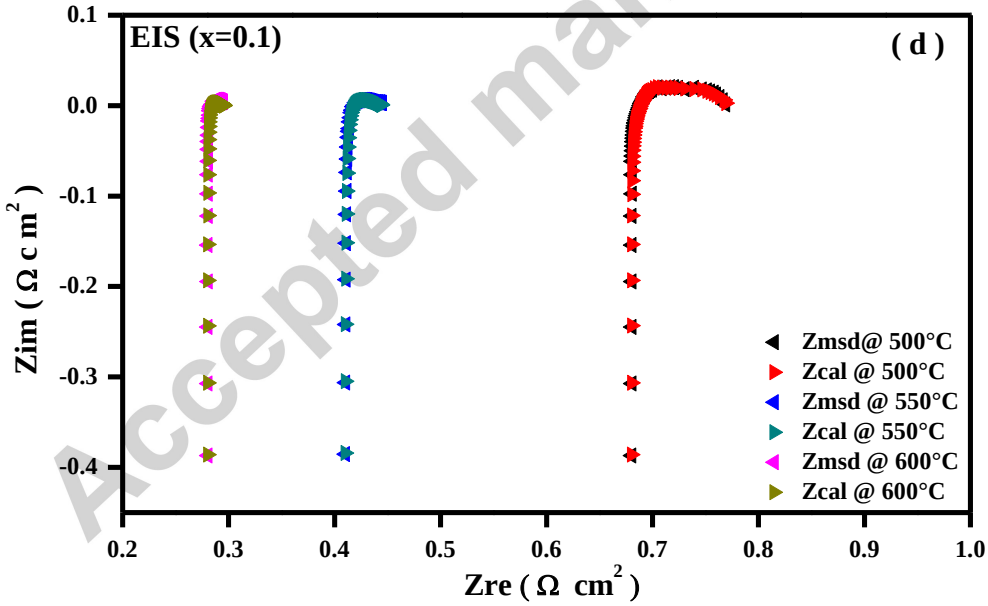

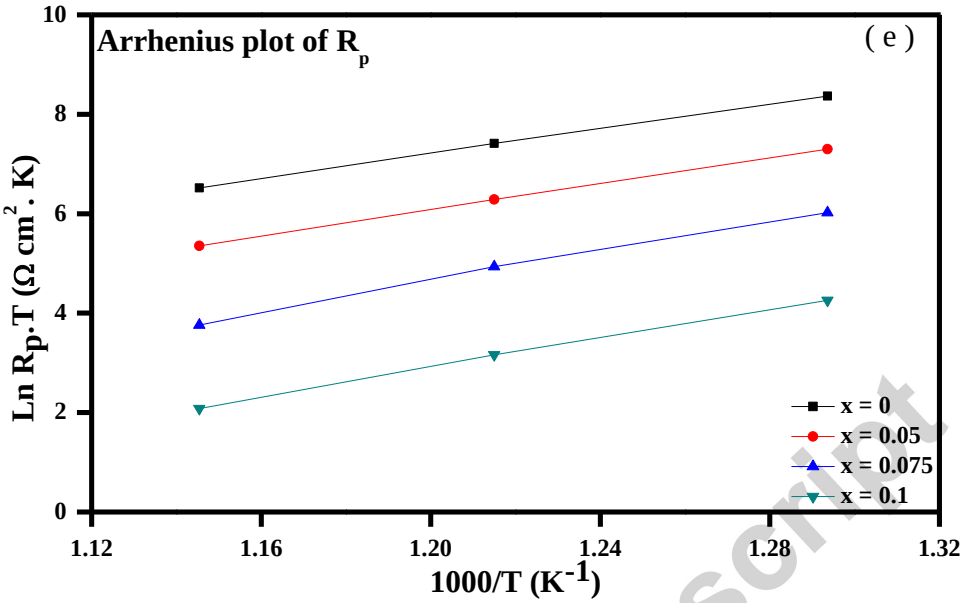

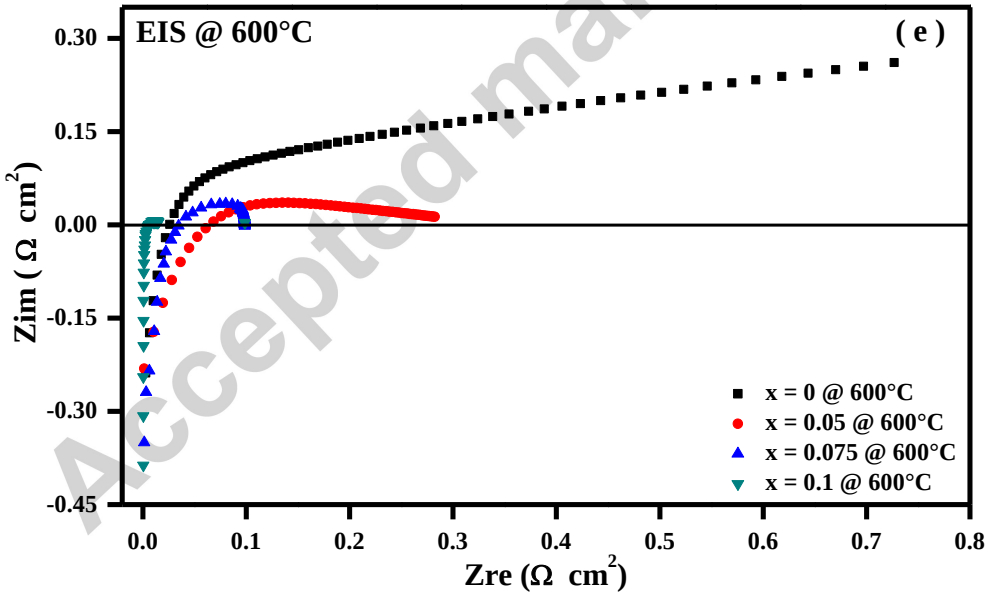

(g)

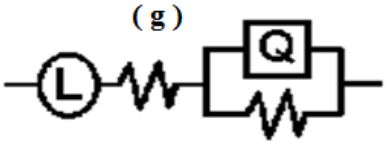

Fig. 5 (a - d) Nyqust plot Electrochemical Impedance Spectroscopy (EIS) in frequency range of 0.1Hz- 1MHz as a function of temperature for $SrFe_{1-x}Ti_xO_{3-\delta}$ (x < = 0.1), (e) Arrhenius plot of

polarization resistance, (f) Nyqust plot for comparison of all the compositions at 600˚C, (g) Equivalent circuit of EIS data calculated by Zsimpwin software.

3.4 Fuel Cell Performance

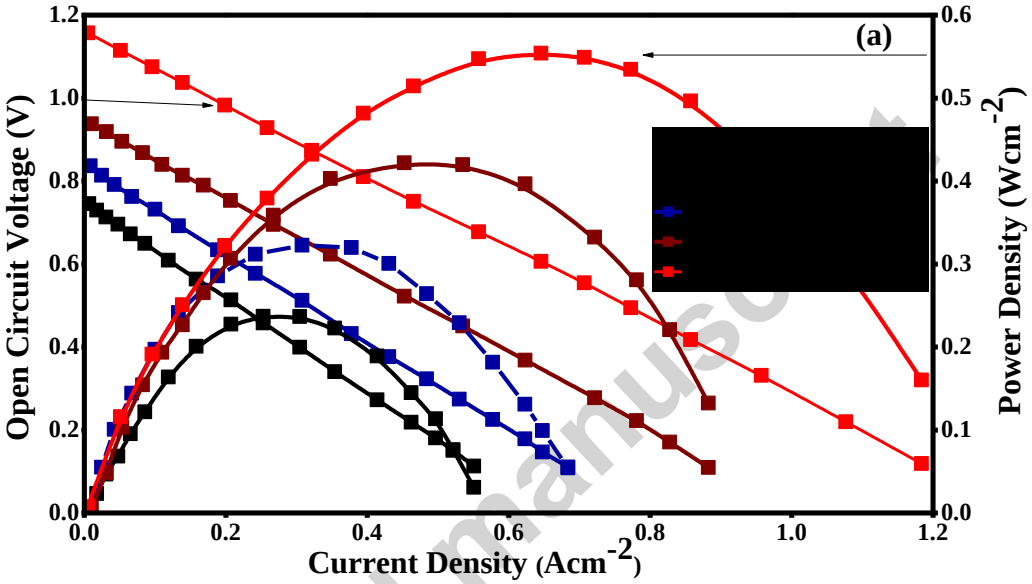

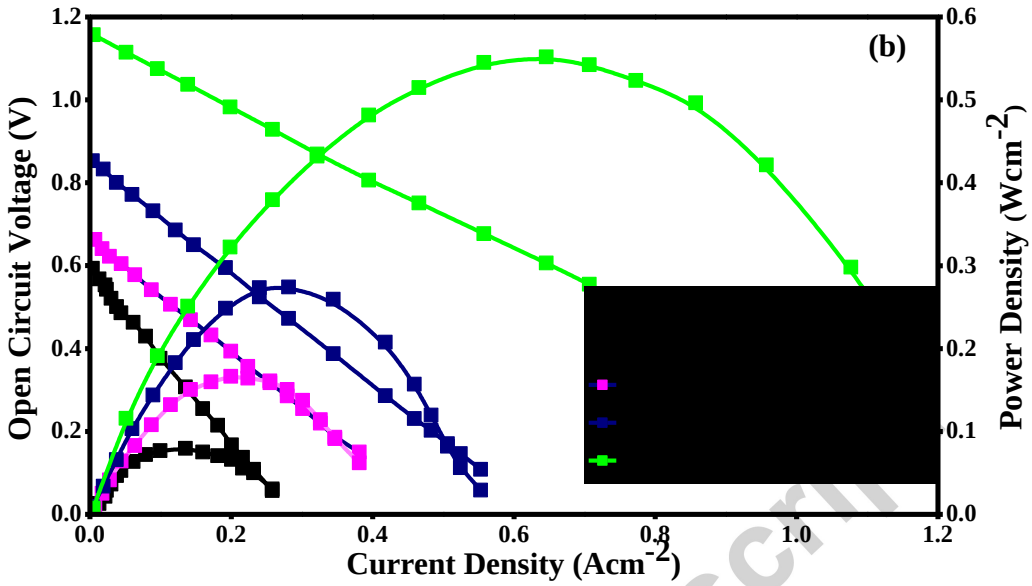

Fig. 6 (a) Typical I-V and I-P characteristics for fuel cells with the $SrFe_{1-x}Ti_xO_{3-\delta}$ (x< = 0.1) cathodes at 600◦C, (b) Fuel cell performance for $SrFe_{0.9}Ti_{0.1}O_{3-\delta}$ cathode at various temperatures

Tables

Table 1 Space group, lattice parameters and unit volume cell parameters refinements of $SrFe_{1-x}Ti_xO_{3-\delta}$ (x < = 0.1)

	$SrFeO_{3-\delta}$	$SrFe_{0.95}Ti_{0.05}O_{3-\delta}$	$SrFe_{0.925}Ti_{0.075}O_{3-\delta}$	$SrFe_{0.9}Ti_{0.1}O_{3-\delta}$
Space group	pm-3m	pm-3m	pm-3m	pm-3m
a (Å)	3.86405	3.8751	3.8850	3.89605
V ($Å^3$)	57.9	59.18	60.4	63.1

Table 2 Brunaurr-Emmett-Teller (BET), results for pore size, surface area and particle size

Sample	pore size m^2/g	BET surface area m^2/g	particle size µm
$SrFeO_{3-\delta}$	0.862	0.8786	2.57
$SrFe_{0.95}Ti_{0.05}O_{3-\delta}$	1.4067	1.4527	0.95
$SrFe_{0.925}Ti_{0.075}O_{3-\delta}$	1.7269	1.7735	0.32
$SrFe_{0.9}Ti_{0.1}O_{3-\delta}$	2.5757	2.6232	0.154

Table 3a Summary of fitted EIS results at 600 °C temperatures for $SrFe_{1-x}Ti_xO_{3-\delta}$ (x < = 0.1)

Ti Contents	Inductance (Henry)	R_{ohmic} (ohm)	R_p (ohm)	CPE (Q)	n	% error
x = 0	8.41E-15	0.31	0.62	101.3	0.8	18.0
x = 0.05	1.196E-15	0.28	0.28	101E-5	0.54	16.0
x = 0.075	4.653E-15	0.25	0.096	5.563E-5	0.45	12.8
x = 0.1	1E-15	0.29	0.01	5.323E-8	0.3	8.0

Table 3b Comparison of polarization (Rp) and area specific (ASR) resistances in typical Ti contents containing cathodes.

Cathode material	Operating Temperature	Rp (Ωcm^2)	ASR (Ωcm^2)	Reference
$Ba_{0.5}Sr_{0.5}Fe_{0.8}Cu_{0.1}Ti_{0.1}O_{3-\delta}$	800^oC	-	0.088	[33]
$SrTi_{0.3}Fe_{0.7}O_{3-\delta}$	$800^oC/H_2$	0.39	-	[34]
$Sr_2FeTi_{6-\delta}$	700^oC	-	0.204	[35]
$SrFe_{0.9}Ti_{0.1}O_{3-\delta}$	600^oC	-	0.16	[36]
$SrFe_{0.95}Ti_{0.05}O_{3-\delta}$	700^oC	-	0.22	[37]
$SrFe_{0.9}Ti_{0.1}O_{3-\delta}$	600^oC	0.01	-	presented work

Table 4a Summary of fuel cells performances using the $SrFe_{1-x}Ti_xO_{3-\delta}$ ($x <= 0.1$) cathodes at 600^oC.

Cathode material	Open circuit voltage (OCV)	Peak power density (P_{max})
$SrFeO_{3-\delta}$	0.74 (Volts)	236 ($mWcm^{-2}$)
$SrFe_{0.95}Ti_{0.05}O_{3-\delta}$	0.83 (Volts)	322 ($mWcm^{-2}$)
$SrFe_{0.925}Ti_{0.075}O_{3-\delta}$	0.94 (Volts)	400 ($mWcm^{-2}$)
$SrFe_{0.9}Ti_{0.1}O_{3-\delta}$	1.15 (Volts)	551 ($mWcm^{-2}$)

Table 4b Comparison of $SrFe_{0.9}Ti_{0.1}O_{3-\delta}$ cathode with different Titanium contents in literature**.**

Cathode materials	Temperature	Peak power density	Reference
$Ba_{0.5}Sr_{0.5}Fe_{0.8}Cu_{0.1}Ti0_{.1}O_{3-\delta}$	800°C	480 (mWcm^{-2})	[33]
$SrTi_{0.3}Fe_{0.7}O_{3-\delta}$	800°C	337 (mWcm^{-2})	[34]
$Sr_2FeTi_{6-\delta}$	800°C	441 (mWcm^{-2})	[35]
$SrFe_{1-x}Ti_xO_{3-\delta}$ (x=0-0.15)	800°C	475-432 (mWcm^{-2})	[36]
$SrFe_{0.95}Ti_{0.05}O_{3-\delta}$+ 20% SDC	800°C	513 (mWcm^{-2})	[37]
$SrFe_{0.9}Ti_{0.1}O_{3-\delta}$	600 ^{o}C	551(mWcm^{-2})	presented work